Electronic Supplementary Information (ESI)

belonging to the communication

An unprecedented heterotrimetallic Fe/Cu/Co core for mild and highly efficient catalytic oxidation of cycloalkanes by hydrogen peroxide

Dmytro S. Nesterov,[a] Volodymyr N. Kokozay,*[a] Viktoriya V. Dyakonenko,[b] Oleg V. Shishkin,[b] Julia Jezierska,[c] Andrew Ozarowski,[d] Alexander M. Kirillov,[e] Maximilian N. Kopylovich[e] and Armando J. L. Pombeiro*[e]

_____

[a] *Department of Inorganic Chemistry, National Taras Shevchenko University, Volodymyrska str. 64, Kyiv 01033, Ukraine. Fax: +38044 2862467; E-mail: kokozay@univ.kiev.ua*

[b] *STC "Institute for Single Crystals "National Academy of Sciences of Ukraine, 60 Lenina ave., Kharkiv 61001, Ukraine.*

[c] *Faculty of Chemistry, University of Wroclaw, 14 Joliot-Curie Str., 50-383 Wroclaw, Poland.*

[d] *National High Magnetic Field Laboratory, Florida State University, 1800 E. Paul Dirac Drive,Tallahassee, Florida 32310, USA.*

[e] *Centro de Química Estrutural, Complexo I, Instituto Superior Técnico, Av. Rovisco Pais, 1049-001, Lisbon, Portugal. Fax: +351 218464455; E-mail: pombeiro@ist.utl.pt*

1. Preparative procedure and characterization details for compound 1

General procedures: C, H and N elemental analyses were carried out by a Carlo Erba Strumentazion Analyzer at the L.V. Pisarzhevskii Institute of Physical Chemistry (Kyiv, Ukraine). Infrared spectra (4000–400 cm^{-1}) were recorded on a Jasco FT/IR–430 instrument in KBr pellets. Differential thermal analysis was conducted in air at a Q–1500 D Paulik-Paulik-Erdey derivatograph with a heating rate of 10 deg/min. A sample of 0.0800 g was heated from ambient temperature up to 800 ^{o}C. For comparative catalytic activity studies, complexes **1a** and **1b** were prepared as previosly reported [D. S. Nesterov, V. G. Makhankova, O. Yu. Vassilyeva, V. N. Kokozay, L. A. Kovbasyuk, B. W. Skelton, J. Jezierska, *Inorg. Chem.* **2004**, *43*, 7868].

General synthetic method: The so-called "direct synthesis of coordination compounds" based on the self-assembly of building blocks, generated *in situ*, into crystalline materials, has been applied for the preparation of **1**. It eliminates the separate step of building block construction and results in a high yield.

Synthesis of 1: Copper powder (0.16 g, 2.5 mmol), Co(NCS)$_2$·2H$_2$O (0.53 g, 2.5 mmol), FeCl$_3$·6H$_2$O (0.68 g, 2.5 mmol), MeOH (30 mL) and diethanolamine (2 mL) were heated to 50–60 °C and stirred magnetically until complete dissolution of copper was observed (1 hour). The resulting solution was filtered. Dark-green crystals of [FeCuCo(L)$_3$(NCS)$_2$(MeOH)]$_2$·5MeOH·H$_2$O (**1′**) suitable for single crystal X-ray analysis deposited from the dark-green filtered solution after successive additions of Pr^{i}OH. They were filtered off and washed with MeOH. The crystals of **1′** are extremely sensitive to loss of solvent of crystallization and easily absorb moisture if exposed in air to give **1** (M = 1329.5) with preservation of the coordination entity. Thus, all studies were performed on powder samples except the X-ray diffraction analysis. The water content may vary slightly among different samples. Yield: 0.8 g, 48.1% (based on copper). Anal. calcd for C$_{30}$H$_{68.4}$Co$_2$Cu$_2$Fe$_2$N$_{10}$O$_{17.2}$S$_4$: Cu, 9.56; Co, 8.87; Fe, 8.40; C, 27.10; H, 5.19; N, 10.53. Found: Cu, 9.2; Co, 9.0; Fe, 8.5; C, 26.89; H, 5.09; N, 10.78. IR (KBr, cm^{-1}): 3450 s br ν(H$_2$O+OH), 3199 s br ν(NH), 2925 s ν$_{as}$(CH), 2881 s ν$_s$(CH), 2141 and 2071 vs ν(CN), 1454 m δ(CH), 1042 s ν(CO), 879 and 814 w ν(CS).

Prediction of the structure: In order to predict the overall configuration of the novel Cu/Co/Fe core we have utilized few simple geometrical considerations described below. The starting point was the known fact that the [Co(L)$_2$]$^-$ subunit possesses an almost regular octahedral geometry. In general this monoanion can combine up to three different metal centers (employing one of the oxygen atoms in a μ$_3$-O coordination mode). However, in **1′** the presence of all metals in the equimolar

ratio suggests that copper and iron polyhedra are consecutively bridged through the [Co(L)$_2$] octahedron. Taking into account the facial coordination mode of the diethanolamine ligand, one can predict the intermetallic Cu–Co–Fe angle to be close to 120°, which represents the theoretical value for the combination of three regular octahedra fused via common edges. The real angle of 101.9° Fig. S1) is in conformity with the values observed earlier for comparable structures with Cu/Co/Cd (111.4°) [D. S. Nesterov, V. G. Makhankova, O. Yu. Vassilyeva, V. N. Kokozay, L. A. Kovbasyuk, B. W. Skelton, J. Jezierska, *Inorg. Chem.* 2004, *43*, 7868] and Cu/Co/Zn (107.6°) [D. S. Nesterov, V. N. Kokozay, B. W. Skelton, *Acta Cryst.* 2006, C**62**, m246] cores.

The IR and DTA characterization: The IR spectrum of **1** (Fig. S8) exhibits a broad ν(H$_2$O+OH) band at 3450 cm^{-1} associated with lattice water and ligated methanol, as well as a set of strong stretching NH (3199 cm^{-1}), CH (2925, 2881 cm^{-1}) and CO (1042 cm^{-1}) vibrations of diethanolamine moieties. The very intense ν(CN) (2141 and 2071cm^{-1}) and weak ν(CS) absorptions (814 and 879 cm^{-1}), typical for the terminal N-bonded thiocyanate ligands, are also observed. The differential thermal analysis curve of compound **1** reveals six exothermic processes over the 70−800°C temperature range (Fig. S9), involving the sequential elimination of the solvated water (70−170°C), of the methanol (170−200°C) and the thiocyanate (200−285°C) ligands, and of four (285−410°C) and two (410−600°C) coupled diethanolamine fragments, to yield (upon complete decomposition ending at 800°C) presumably a spinel-type heterotrimetallic oxide Cu(FeCo)O$_4$. The observed mass losses at the different stages of thermolysis agree with those calculated according to this decomposition scheme, which is also supported by the IR spectra of remaining products recorded after each thermal effect (Fig. S8). In general, the thermal behaviour of **1** exhibits an oxidative character being typical for other Cu and Co complexes with resembling ligands [V. T. Yilmaz, Y. Topcu, F. Yilmaz, C. Thoene, *Polyhedron* 2001, **20**, 3209; A. Karadag, V. T. Yilmaz, C. Thoene, *Polyhedron* 2001, **20**, 635].

The magnetic susceptibility measurements and EPR spectroscopy data: The EPR spectrum of compound **1** at 5 K and at 195 GHz (inset in Fig. S6) is characteristic of a monomeric Cu^{II} center, with g$_x$=2.042, g$_y$=2.058, g$_z$=2.303, while at higher temperatures a broad unresolved line appears with g close to 2.02 which is likely to be due to the exchange-coupled system. The molecular structure suggests that to the first approximation only the two Fe^{III} high spin ions are involved in

exchange interactions, which may be described by the spin Hamiltonian $H=J_{FeFe}S_{Fe1}S_{Fe2}$. With such assumption, the magnetic susceptibility of the Fe_2Cu_2 system may be expressed as the sum of paramagnetic susceptibility due to two isolated copper ions plus the susceptibility of a coupled pair of iron ions. However, this approximation resulted in not a very good fit and in unacceptably high values of g_{Fe}=2.11 and g_{Cu}=2.47, while J_{FeFe} was 28 cm^{-1}. The failure of the model indicates that the interaction Fe-Cu may not be negligible. Another source of error was neglecting the zero-field splitting on Fe^{III} ions that may be comparable to the exchange integrals and could affect magnetic susceptibilities. Therefore, the spin Hamiltonian operator for the system was extended to the form

$H = J_{FeFe}S_{Fe1}S_{Fe2} + J_{CuFe}(S_{Fe1}S_{Cu1}+S_{Fe2}S_{Cu2}) + J'_{CuFe}(S_{Fe1}S_{Cu2}+S_{Fe2}S_{Cu1}) +$

$D_{Fe}[S_{zFe1}{}^2-(1/3)S_{Fe1}(S_{Fe1}+1)] + D_{Fe}[S_{zFe2}{}^2-(1/3)S_{Fe2}(S_{Fe2}+1)] +$

$\mu_B Bg_{Fe}(S_{Fe1} + S_{Fe2}) + \mu_B Bg_{Cu}(S_{Cu1} + S_{Cu2})$ (1)

where J_{CuFe} represents interaction of iron atom with the copper atom closer to it, while J'_{CuFe} represents the interaction of iron and copper atoms located in different halves of the molecule. The least-squares fitting procedure evaluated all 144 energies of the $|S,Ms\rangle$ states in the system by full diagonalisation of the 144x144 matrix of the spin Hamiltonian. The susceptibility was then calculated from the formula

$$\chi = -\frac{N}{B}\frac{\sum_{i=1}^{144}\frac{\partial E_i}{\partial B}\exp(-E_i/kT)}{\sum_{i=1}^{144}\exp(-E_i/kT)} + TIP \qquad (2)$$

in which the derivatives $\delta E_i/\delta B$ had to be evaluated numerically. The g_{Cu} value was assumed equal to $g_{average}$ = 2.134 as found from EPR, g_{Fe} was assumed to be equal to 2.0 and the value of TIP= $120\cdot10^{-6}$ cgs emu was used. Other parameters of Hamiltonian (1) were fitted resulting in D_{Fe}= -8.5 cm^{-1}, J_{FeCu} = -7.9 cm^{-1}, J'_{FeCu} = -7.0 cm^{-1}, J_{FeFe} = 27.3 cm^{-1} (see Fig. S6). The J_{FeFe} magnitude is quite typical for alkoxo-bridged iron(III) pairs [M. Kato, Y. Yamada, T. Inagaki, W. Mori, K. Sakai, T. Tsubomura, M. Sato, S. Yano *Inorg. Chem.*1995, **34**, 2645] (Note that exchange Hamiltonian in that paper was used in the form H=-2$J_{FeFe}S_{Fe1}S_{Fe2}$). The interactions between iron and copper ions may seem large, as these ions must interact through diamagnetic cobalt(III) ions. However, diamagnetic metal atoms have been found to transmit exchange interactions surprisingly efficiently [E. A. Buvaylo; V. N. Kokozay, O. Yu. Vassilyeva, B. Skelton, J. Jezierska, L. C. Brunel, A. Ozarowski, *Chem. Commun.* 2005, **39**, 4976 and references therein].

2. Details of the X-ray crystal structure analysis and refinement

Diffraction experiments were performed on a Xcalibur-3 diffractometer (CCD-detector, ω scanning, $2\theta_{max} = 50°$) equipped with graphite monochromated Mo-Kα radiation ($\lambda = 0.71073$ Å). The data were corrected for the absorption using multi-scan method [CrysAlis RED, Oxford Diffraction Ltd., Version 1.171.29.9 (release 23-03-2006 CrysAlis171.NET) (compiled Mar 23 2006, 23:39:28); empirical absorption correction using spherical harmonics, implemented in SCALE3 ABSPACK scaling algorithm] with min./max. transmission factors of 0.58/0.68. The structure was solved by direct methods and refined by full-matrix least-squares methods against F^2 using SHELX97 program [Sheldrick G.M. *SHELX97. PC Version. A system of computer programs for the crystal structure solution and refinement.* Rev. 2. 1998]. In general the non-hydrogen atoms were refined anisotropically. The metal assignment was based on refinement. Positions of hydrogen atoms were located from electron density difference maps and refined by riding model with $U_{iso} = nU_{eq}$ (n = 1.5 for methyl group and n = 1.2 for other hydrogen atoms). One of the thiocyanate group [N(5), C(15), S(2)] was modeled as being disordered, the populations of the two components refining to 0.790(10) and 0.210(10). The C(2) and C(4) atoms of the diethanolamine ligand were found to be disordered; the two sets of sites [C(2A), C(4A) and C(2B), C(4B)] have site occupancies of 0.464(8) and 0.536(8), respectively. The disordered section of solvents have primed [O(3SA), C(3SA); O(1W)] and unprimed [O(3SB), C(3SB); O(4S), C(4S)] components, each assigned populations of 0.5. The minor component of the water molecule was not located. The carbon atom C(2S) of the methanol molecule was found to be disordered over two sites of equal occupancy.

3. Experimental details of magnetic studies

High-frequency EPR spectra were recorded on a home-built spectrometer at the EMR facility of NHMFL [A. K. Hassan, L. A. Pardi, J. Krzystek, A. Sienkiewicz, P. Goy, M. Rohrer, L.-C. Brunel. *J. Magn. Reson.* 2000, **142**, 300]. The instrument was a transmission-type device in which waves are propagated in cylindrical lightpipes. The microwaves were generated by a Gunn oscillator, operating at 95 ± 3 GHz. Frequencies higher by a factor 2, 3, or 4 were obtained using a Schottky diode-based multiplier and appropriate high-pass filters. A phase-locked oscillator (Virginia Diodes) generating frequency of 52 ± 4 GHz and its 2nd, 4th and 6th harmonics was also used. A superconducting magnet (Oxford Instruments) capable of reaching a field of 17 T was employed.

Magnetic susceptibility data of a powdered sample were measured with a SQUID magnetometer (Quantum Design MPMSXL-5) over the temperature range 1.8–300 K at the magnetic induction of 0.5 T. Corrections for the sample holders were applied. Diamagnetic corrections for the molecule (522·10[-6] cgs emu) were determined from Pascal's constants.

4. Experimental details of catalytic activity studies

The reaction mixtures were prepared as follows: to 0.63−20.0 µmol (typically 10.0 µmol) of catalyst (complex **1**) contained in the reaction flask were added 0.0−9.0 mL (typically 4.5 mL) MeCN, 0.0−0.6 mmol (typically 0.2 mmol) HNO_3, 1.0 mmol of cycloalkane and 1.00−20.0 mmol (typically 5.00 mmol) H_2O_2 (30 % in H_2O), in this order. The reaction mixture was stirred for 2−24 h at room temperature and atmospheric pressure, then 90 µL of cycloheptanone (as internal standard), 4.00−13.0 mL (typically 8.50 mL) diethyl ether (to extract the substrate and the products from the reaction mixture) and 1.0 g PPh_3 (to reduce organo-hydroperoxides if formed) were added. The resulting mixture was stirred for 15 min and then a sample taken from the organic phase was analyzed by GC using a FISONS Instruments GC 8000 series gas chromatograph with a DB WAX fused silica capillary column (P/N 123-7032) and the Jasco-Borwin v.1.50 software. In some cases, the products were also identified by GC-MS technique using a Trio 2000 Fisons spectrometer with a coupled Carlo Erba (Auto/HRGC/MS) gas chromatograph. The GC analyses of the aqueous phase showed the presence of only traces (less than 0.05 %) of oxidation products. In the experiments with radical traps, the appropriate compounds e.g. 2,6-di-tert-butyl-4-methylphenol (BHT), $CBrCl_3$ or Ph_2NH (2.5 mmol) were also added to the reaction mixture.

Blank experiments were performed for both cycloalkanes with different amounts of H_2O_2 and other reagents, and confirmed that no alkane oxidation products (or only traces, below 0.3%) were obtained in the absence of the metal catalyst.

Compound **1**, under the above catalytic experimental conditions but in the absence of the cycloalkane, gradually converts into other unidentified and much less active species. A substantial product yield drop also occurs if the cycloalkane is not added immediately to the catalytic reaction solution, as indicated above, corroborating the instability of the active species.

5. Supporting schemes, X-ray figures, magnetic susceptibility plot, EPR spectra and thermal analysis data for 1. Selected bonding parameters and hydrogen bond geometry in complex 1
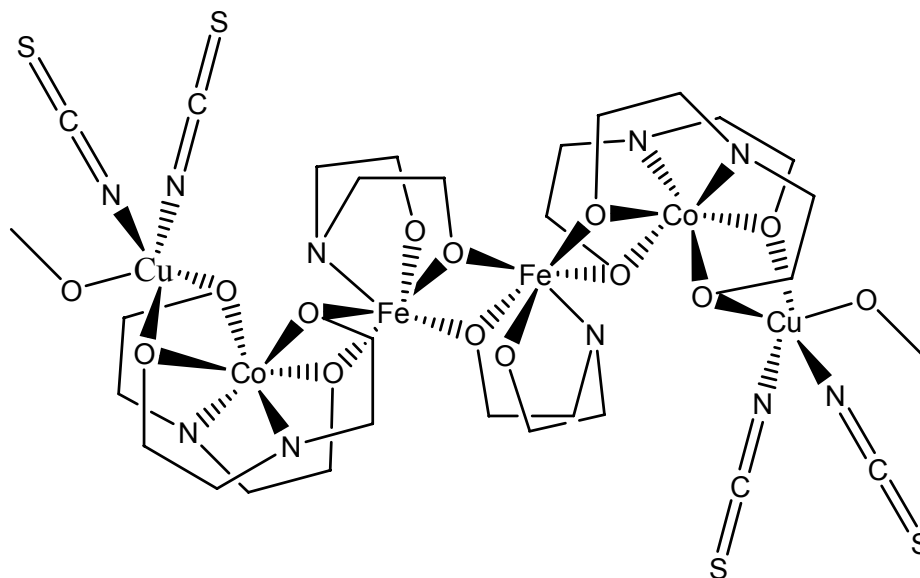
Scheme S1. Schematic representation of the molecular structure of **1** (crystallization water, NH and MeOH protons are not shown).
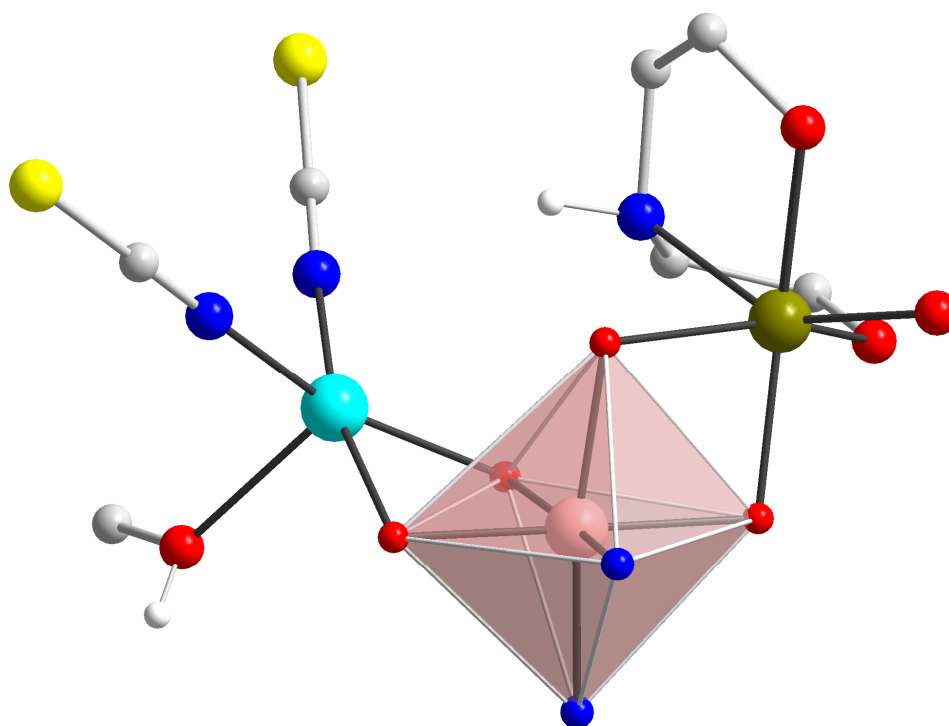

Figure S1. Schematic partial representation of the linkage of copper and iron centers through the cobalt octahedron in **1′** forming a heterotrimetallic $Cu(\mu\text{-}O)_2Co(\mu\text{-}O)_2Fe$ core. Fe greenish brown, Cu light-blue, Co pink, O red, N blue, S yellow, C grey, H white.
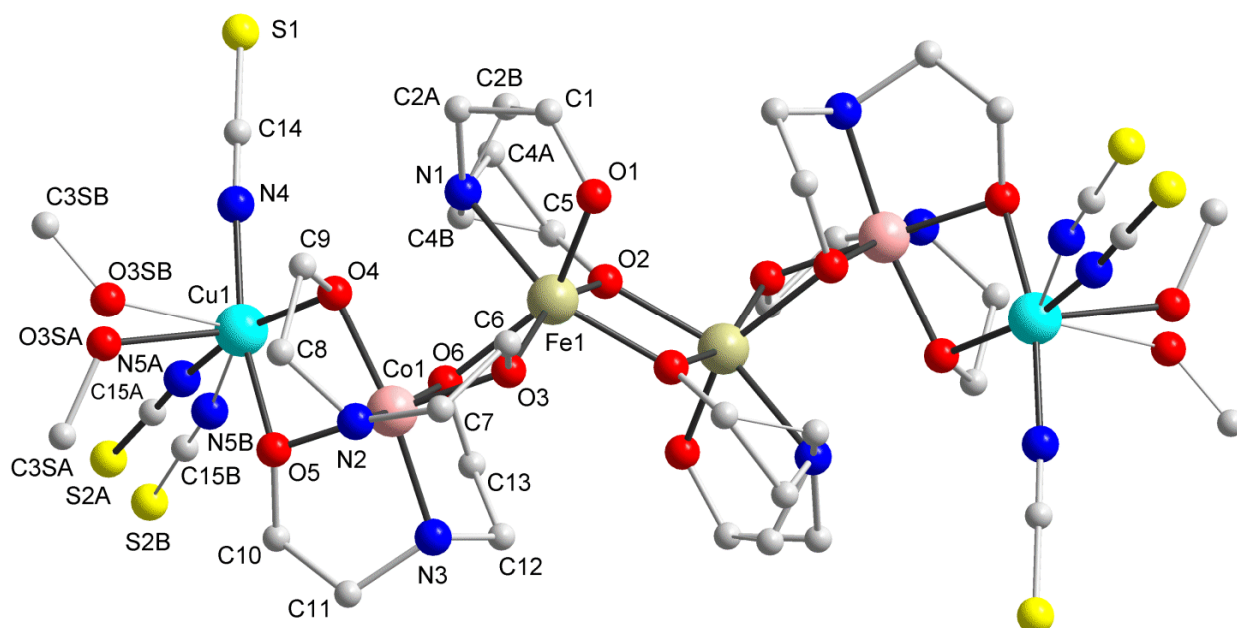
Figure S2. Ball-and-stick representation of the molecular structure of **1′** with the numbering scheme. The uncoordinated methanol molecules and hydrogen atoms are omitted for clarity. Fe greenish brown, Cu light-blue, Co pink, O red, N blue, S yellow, C grey, H white.
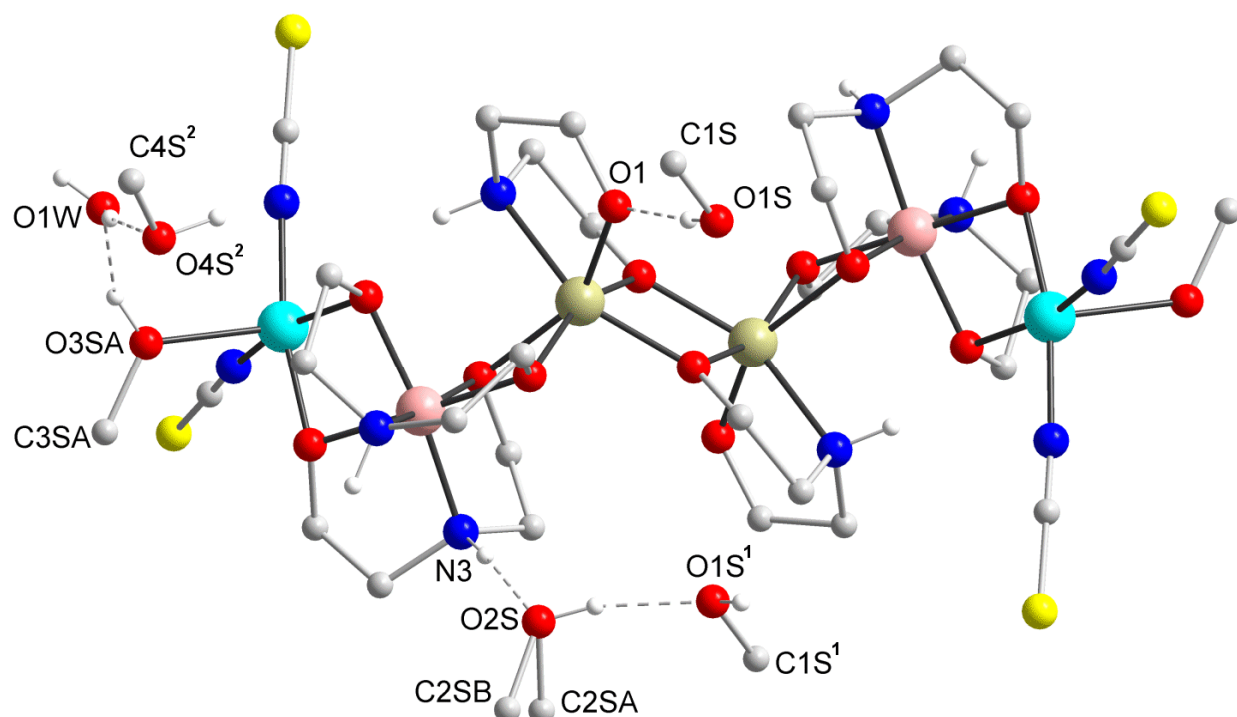

Figure S3. The hydrogen-bonding scheme in **1′** (hydrogen atoms from the CH_2 groups and minor components of the disordered thiocyanate and CH_2 groups are omitted for clarity) showing the primed components of the disordered solvents, symmetry transformations used: [1] 2–x, 1–y, –z; [2] 2–x, 2–y, 1–z. Fe greenish brown, Cu light-blue, Co pink, O red, N blue, S yellow, C grey, H white.
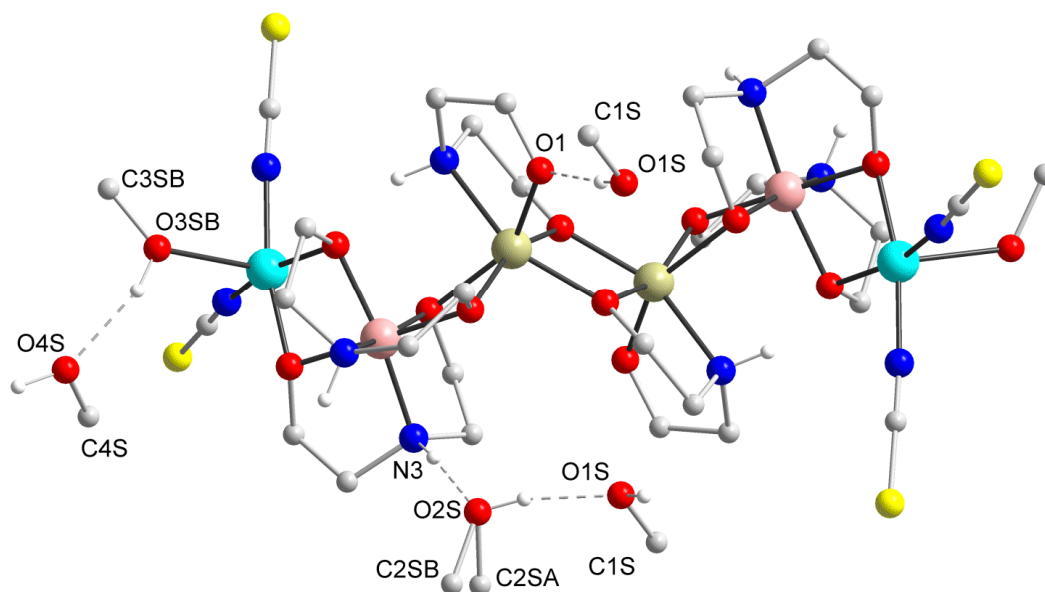
Figure S4. The hydrogen-bonding scheme in **1′** (hydrogen atoms from the CH₂ groups and minor components of the disordered thiocyanate and CH₂ groups are omitted for clarity) showing the unprimed components of the disordered solvents. Fe greenish brown, Cu light-blue, Co pink, O red, N blue, S yellow, C grey, H white.
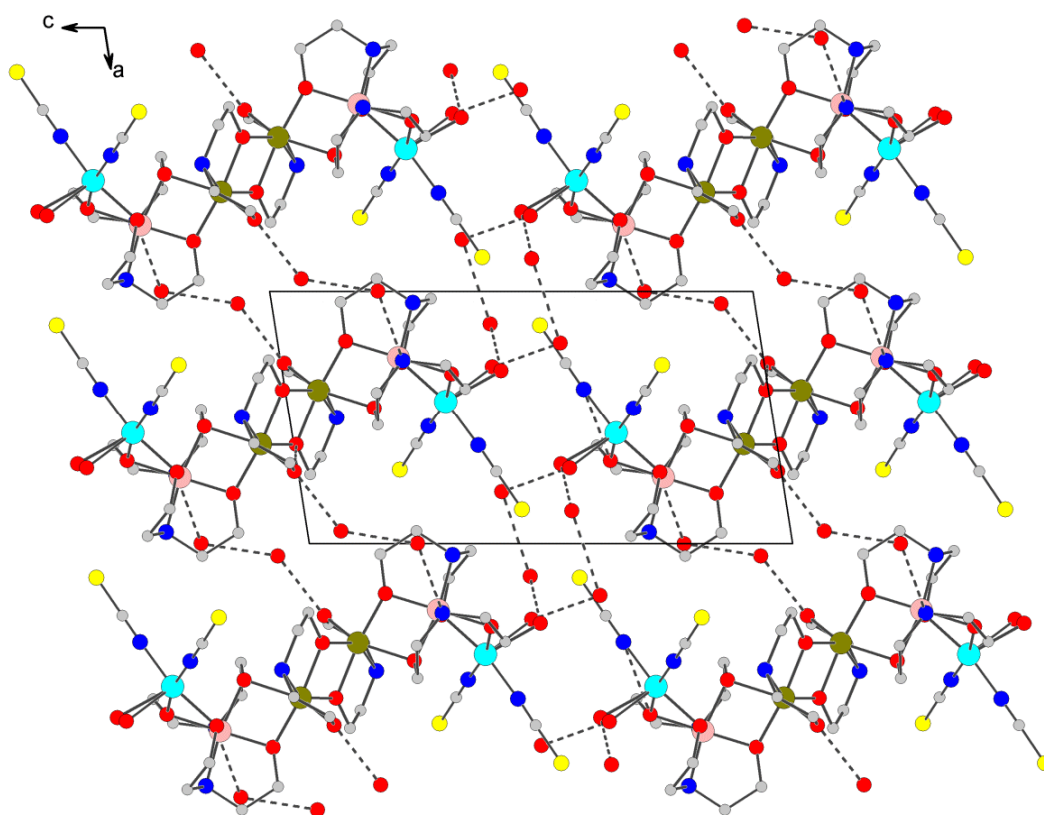

Figure S5. Projection of the hydrogen-bonded layer in **1′** on the *ac* plane (hydrogen atoms and carbon atoms of methanol molecules are omitted for clarity). Fe greenish brown, Cu light-blue, Co pink, O red, N blue, S yellow, C grey.
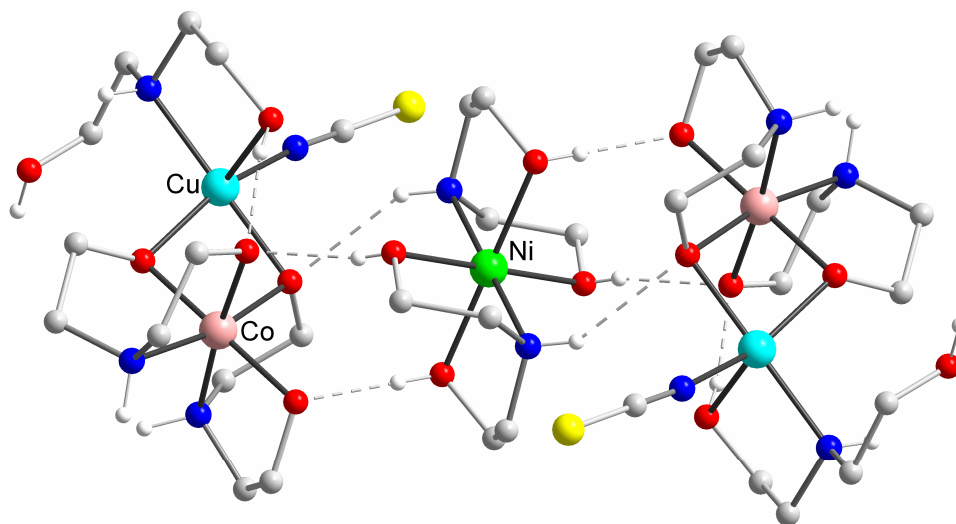
Figure S6. Ball-and-stick representation of the molecular structure of **2a** (for comparative purposes). The hydrogen atoms from the CH$_2$ groups as well as uncoordinated NCS$^-$ groups are omitted for clarity. Ni green, Cu light-blue, Co pink, O red, N blue, S yellow, C grey, H white.
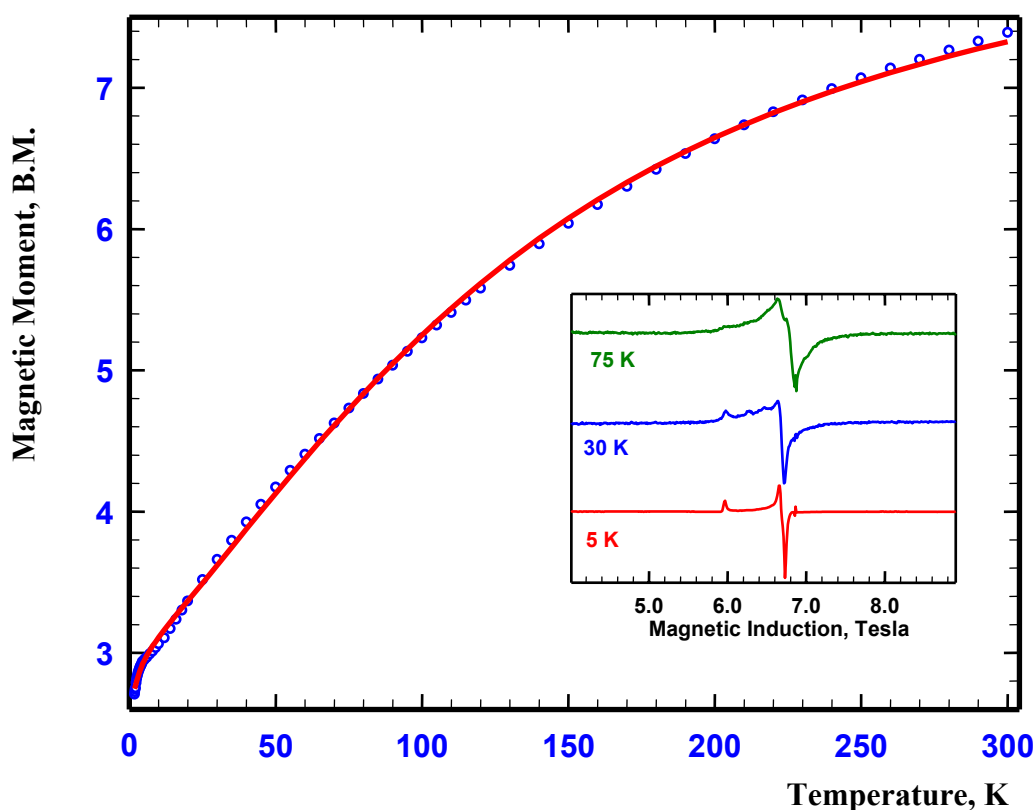
Figure S7. Plot of the magnetic moment per molecule *versus* temperature for complex **1**. The solid line was calculated from equation (2) with $g_{Cu}= 2.134$, $g_{Fe}= 2.00$, $D_{Fe}= -8.5 cm^{-1}$, TIP= $120 \cdot 10^{-6}$ cgs emu, $J_{FeCu} = -7.9 cm^{-1}$, $J'_{FeCu} = -7.0 cm^{-1}$, $J_{FeFe} = 27.3 cm^{-1}$. The inset shows EPR spectra recorded at 192.47 GHz at temperatures indicated.

Figure S8. IR spectra of **1** and its thermolysis products remained after each thermal effect.

Figure S9. Plot of differential thermal analysis of **1**.

Table S1. Results of differential thermal analysis of **1**.

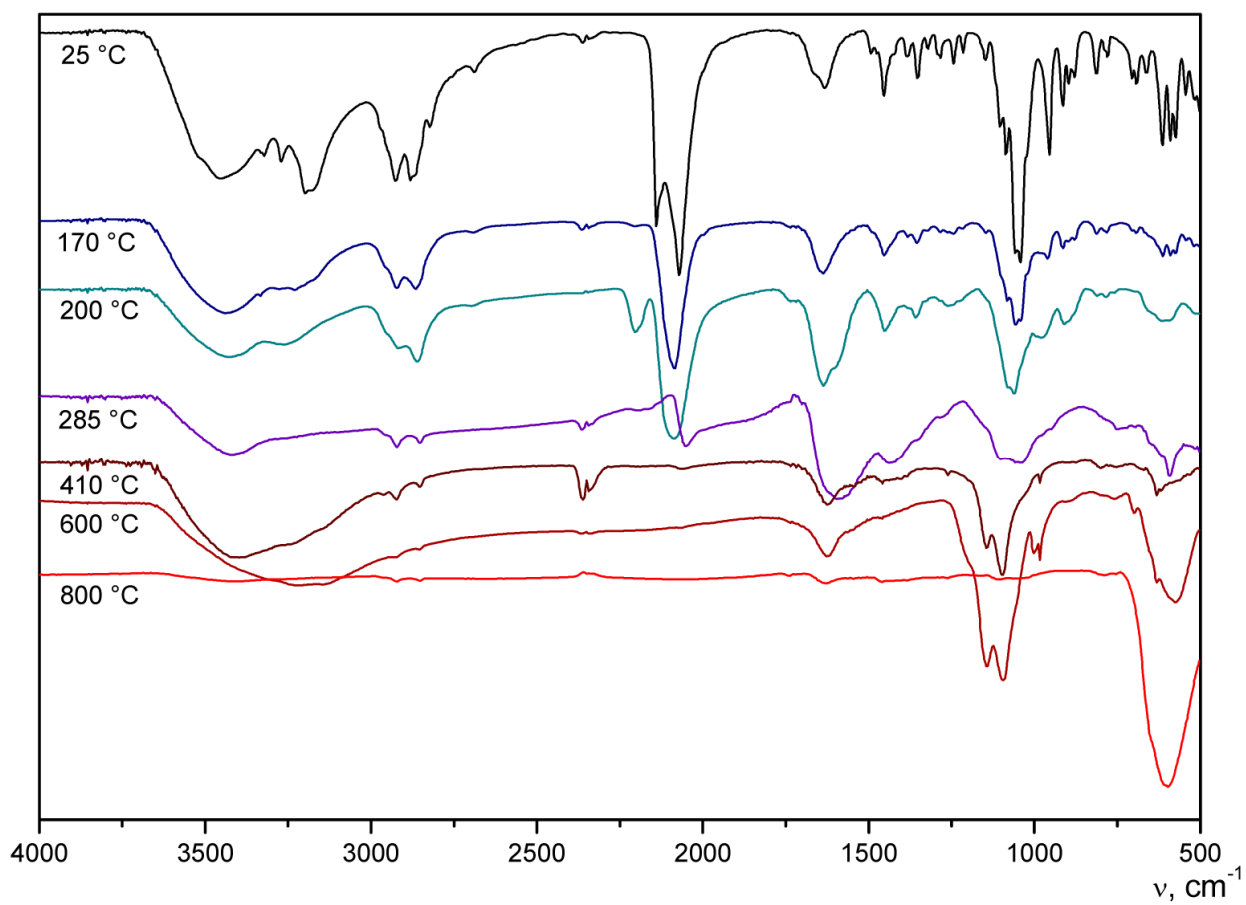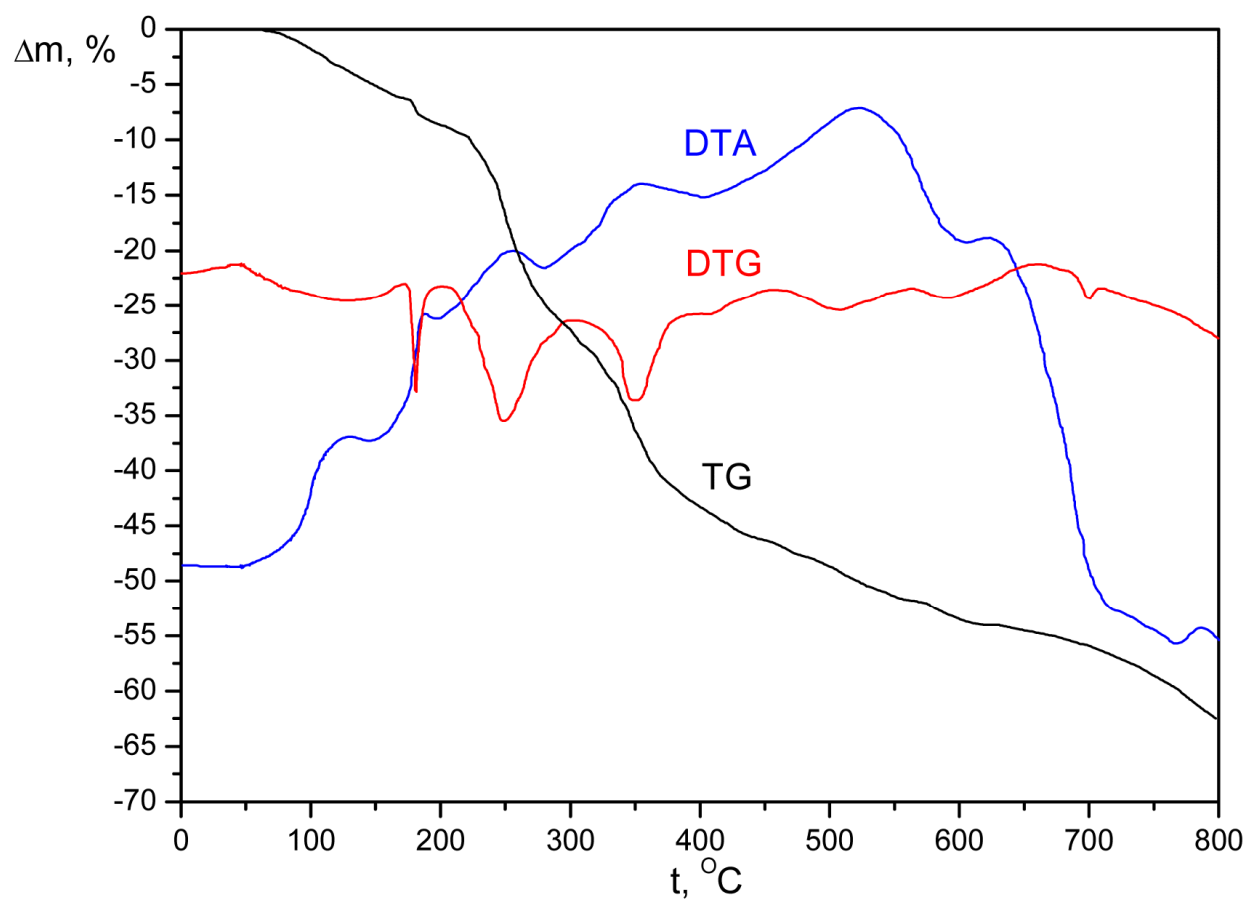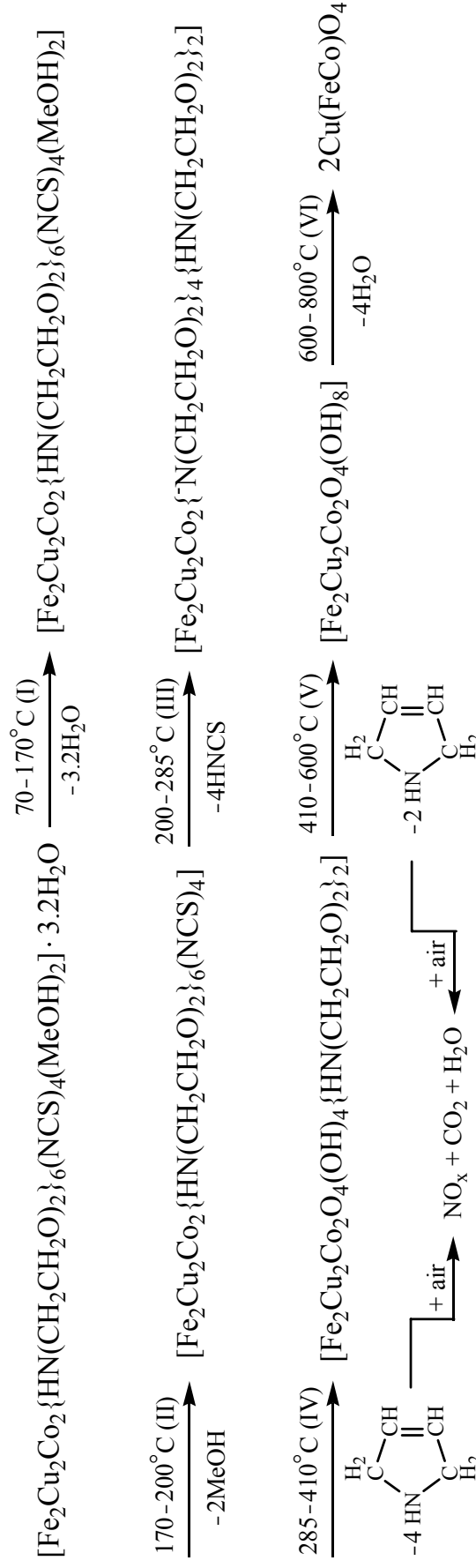| Thermal effect[a]	Temperature, °C		Σ Mass loss, %(mass.)		Species eliminated	Species formed
	interval	maximum(a)	observed	calculated[b]		
I	70–170	130	4.9	4.3	$3.2H_2O$	$[Fe_2Cu_2Co_2\{HN(CH_2CH_2O)_2\}_6(NCS)_4(MeOH)_2]$
II	170–200	180	8.8	9.2	2MeOH	$[Fe_2Cu_2Co_2\{HN(CH_2CH_2O)_2\}_6(NCS)_4]$
III	200–285	250	26.7	26.9	4HNCS	$[Fe_2Cu_2Co_2\{N(CH_2CH_2O)_2\}_4\{HN(CH_2CH_2O)_2\}_2]$
IV	285–410	350, 380	47.1	47.7	$4C_4H_7N$	$[Fe_2Cu_2Co_2O_4(OH)_4\{HN(CH_2CH_2O)_2\}_2]$
V	410–600	520	57.6	58.1	$2C_4H_7N$	$[Fe_2Cu_2Co_2O_4(OH)_8]$
VI	600–800	620, 780	62.5	63.5	$4H_2O$	$2Cu(FeCo)O_4$

[a] Allocation of thermal effects is based on the DTA curve. [b] Based on the proposed species which are eliminated and formed.

$[Fe_2Cu_2Co_2\{HN(CH_2CH_2O)_2\}_6(NCS)_4(MeOH)_2] \cdot 3.2H_2O \xrightarrow[-3.2H_2O]{70-170^\circ C \ (I)} [Fe_2Cu_2Co_2\{HN(CH_2CH_2O)_2\}_6(NCS)_4(MeOH)_2]$

$\xrightarrow[-2MeOH]{170-200^\circ C \ (II)} [Fe_2Cu_2Co_2\{HN(CH_2CH_2O)_2\}_6(NCS)_4] \xrightarrow[-4HNCS]{200-285^\circ C \ (III)} [Fe_2Cu_2Co_2\{N(CH_2CH_2O)_2\}_4\{HN(CH_2CH_2O)_2\}_2]$

$\xrightarrow[]{285-410^\circ C \ (IV)} [Fe_2Cu_2Co_2O_4(OH)_4\{HN(CH_2CH_2O)_2\}_2] \xrightarrow[]{410-600^\circ C \ (V)} [Fe_2Cu_2Co_2O_4(OH)_8] \xrightarrow[-4H_2O]{600-800^\circ C \ (VI)} 2Cu(FeCo)O_4$

Scheme S1. Proposed thermolysis scheme of **1**.

Table S2. Selected bond lengths (Å) and angles (deg) in complex **1′**.[a]

Fe(1)–O(1)	1.926(2)	Cu(1)–N(5B)	2.17(2)
Fe(1)–O(2)[1]	1.971(3)	Cu(1)–O(3SA)	2.248(12)
Fe(1)–O(3)	2.003(2)	Cu(1)–O(3SB)	2.331(8)
Fe(1)–O(2)	2.021(2)	Cu(1)–Co(1)	2.8344(8)
Fe(1)–O(6)	2.090(2)	Co(1)–O(3)	1.881(2)
Fe(1)–N(1)	2.179(3)	Co(1)–O(5)	1.892(3)
Cu(1)–N(5A)	1.922(8)	Co(1)–O(4)	1.907(3)
Cu(1)–N(5)	1.951(5)	Co(1)–O(6)	1.913(2)
Cu(1)–O(5)	1.956(3)	Co(1)–N(3)	1.932(3)
Cu(1)–O(4)	2.006(3)	Co(1)–N(2)	1.941(3)
O(1)–Fe(1)–O(2)[1]	98.48(11)	N(5)–Cu(1)–O(3SA)	102.3(4)
O(1)–Fe(1)–O(3)	93.37(10)	O(5)–Cu(1)–O(3SA)	87.0(3)
O(2)–Fe(1)–O(3)[1]	93.19(10)	O(4)–Cu(1)–O(3SA)	107.1(4)
O(1)–Fe(1)–O(2)	106.77(10)	N(5B)–Cu(1)–O(3SA)	98.4(8)
O(2)–Fe(1)–O(2)[1]	72.52(10)	N(5A)–Cu(1)–O(3SB)	98.0(3)
O(3)–Fe(1)–O(2)	156.60(10)	N(5)–Cu(1)–O(3SB)	88.7(2)
O(1)–Fe(1)–O(6)	149.86(12)	O(5)–Cu(1)–O(3SB)	98.9(2)
O(2)–Fe(1)–O(6)[1]	109.64(11)	O(4)–Cu(1)–O(3SB)	97.8(2)
O(3)–Fe(1)–O(6)	74.90(10)	N(5B)–Cu(1)–O(3SB)	111.3(8)
O(2)–Fe(1)–O(6)	92.19(9)	O(3SA)–Cu(1)–O(3SB)	16.8(3)
O(1)–Fe(1)–N(1)	80.19(11)	O(3)–Co(1)–O(5)	178.81(12)
O(2)–Fe(1)–N(1)[1]	148.56(11)	O(3)–Co(1)–O(4)	96.12(11)
O(3)–Fe(1)–N(1)	118.24(11)	O(5)–Co(1)–O(4)	82.68(13)
O(2)–Fe(1)–N(1)	77.81(11)	O(3)–Co(1)–O(6)	82.03(10)
O(6)–Fe(1)–N(1)	81.28(12)	O(5)–Co(1)–O(6)	98.01(11)
N(5A)–Cu(1)–N(5)	91.9(3)	O(4)–Co(1)–O(6)	88.79(12)
N(5A)–Cu(1)–O(5)	96.2(2)	O(3)–Co(1)–N(3)	93.83(12)
N(5)–Cu(1)–O(5)	167.91(14)	O(5)–Co(1)–N(3)	87.36(14)
N(5A)–Cu(1)–O(4)	164.0(2)	O(4)–Co(1)–N(3)	168.69(13)
N(5)–Cu(1)–O(4)	91.15(14)	O(6)–Co(1)–N(3)	87.27(13)
O(5)–Cu(1)–O(4)	78.60(11)	O(3)–Co(1)–N(2)	87.52(12)
N(5A)–Cu(1)–N(5B)	16.8(7)	O(5)–Co(1)–N(2)	92.33(13)
N(5)–Cu(1)–N(5B)	101.9(7)	O(4)–Co(1)–N(2)	87.31(12)

O(5)–Cu(1)–N(5B)	84.1(7)	O(6)–Co(1)–N(2)	168.39(13)
O(4)–Cu(1)–N(5B)	148.1(8)	N(3)–Co(1)–N(2)	98.50(14)
N(5A)–Cu(1)–O(3SA)	87.5(4)		

[a] Symmetry transformation used to generate equivalent atoms: [1] 1–x, 1–y, –z.

Table S3. Hydrogen bond geometry (Å, °) in complex **1′**.[a]

D–H···A	d(D–H)	d(H···A)	d(D···A)	∠(D–H···A)
O(1S)–H(1O)···O(1)	0.88	1.76	2.63	168.1
O(3SA)–H(3SO)···O(1W)	0.95	1.96	2.84	152.7
N(3)–H(3)···O(2S)	0.93	1.96	2.88	171.1
O(3SB)–H(3S1)···O(4S)	0.95	1.95	2.81	149.2
O(2S)–H(2O)···O(1S)[1]	0.89	1.84	2.71	164.8
O(1W)–H(1WA)···O(4S)[2]	0.85	2.22	3.05	167.9

[a] Symmetry transformation used to generate equivalent atoms: [1] 2–x, 1–y, –z; [2] 2–x, 2–y, 1–z.